S15

DIFFUSE X-RAY SCATTERING FROM GRADED SiGe LAYERS

J. Endres

Department of Condensed Matter Physics, Faculty of Mathematics and Physics, Charles University Prague, Ke Karlovu 5, 121 16 Prague 2, Czech Republic
jan.endres@seznam.cz

Graded SiGe layers are frequently used as virtual substrate for electronic and optoelectronic device applications. The grading makes it possible to make a substrate with lattice constant matched to the device and to decrease the density of threading dislocations crossing the layer and therefore to improve the quality of the layers deposited on the top.

Intensity distribution of scattered X-rays $I(\boldsymbol{Q})$ is measured as the reciprocal space map of the $\boldsymbol{Q}=(Q_x,Q_z)$ plane or along various direction in this plane (the X-ray beams are assumed to be well collimated in the incidence xz plane). The intensity is concentrated around the reciprocal lattice point so that we consider the wave vector deviation $\boldsymbol{q}=\boldsymbol{Q}-\boldsymbol{Q}^0$ ($\boldsymbol{Q}^0$ is the nearest reciprocal lattice vector). In the kinematic approximation, the intensity scattered by the layer with thickness h can be represented as Fourier integral [1]

$$I(\boldsymbol{q}) \quad A \int_V d^3\boldsymbol{r} \int_{V'} d^3\boldsymbol{r}' \exp i\boldsymbol{q}(\boldsymbol{r}-\boldsymbol{r}')\, G(\boldsymbol{r},\boldsymbol{r}') \qquad (1)$$

where A is constant, V (V') is volume of scattering area and

$$G(\boldsymbol{r},\boldsymbol{r}') \quad \left\langle \exp(i\boldsymbol{Q}(\boldsymbol{u}(\boldsymbol{r}) \quad \boldsymbol{u}(\boldsymbol{r}'))) \right\rangle \qquad (2)$$

is correlation function, where $\boldsymbol{u(r)}$ is the displacement at the site $\boldsymbol{r}$ due to randomly distributed dislocations, and the average is performed over their positions. We consider the case of uncorrelated dislocations in two systems, with dislocation lines parallel to x and y axis. Then we can derive [1] approximation of the correlation function. For calculations we need to know the distribution of dislocations in the layer. We can use two models: Tersoff model [2] or model Dodson-Tsao [3].

Tersoff model describes equilibrium distribution of dislocations. The density of dislocations is just enough to exactly cancel the mismatch up to a distance z_c from the interface between layer and substrate and there are no dislocations at all above z_c. The boundary z_c of the dislocation-free region is given by the condition

$$\int_{z_0}^{h} dz \; f(z) \quad f(z_c) \quad \frac{}{bc} \qquad (3)$$

where $f(z)$ is the mismatch between bulk lattice constant $a(z)$ and substrate lattice constant, is energy per unit length of the dislocation, b is length of the Burgers vector of misfit dislocation and c is the appropriate elastic constant. If the layer is graded linearly from the substrate, Equation (3) can be solved analytically and density of dislocations is constant in whole region under z_c.

Dodson-Tsao model describes the kinetics of plastic relaxation in the layer by the equation

$$\frac{d_{\parallel}(z)}{dt} \quad K \quad {}^{2}_{exc}(z) \quad \frac{{}^{2}_{exc}(z)}{} \quad {}_{\parallel}(z) \quad {}_{0} \;, \qquad (4)$$

where ${}_{\parallel}$ is lateral misfit, K is constant, ${}_{exc}$ is excess stress, is a share modulus and ${}_{0}$ is constant, which makes it possible to start plastic relaxation even without presence of misfit dislocations. From the solution of equation (4) the relaxation of the layer $r(z) = {}_{\parallel}(z)/f(z)$ is obtained.

1. V. M. Kaganer, R. Köhler, M. Schmidbauer, R. Opitz, X-ray diffraction peaks due to misfit dislocations in heteroepitaxial structures. *Physical Review B*, **55** (1997) 1793-1810.
2. J. Tersoff, Dislocation and strain relief in compositionally graded layers. *Appl. Phys. Lett.,* **62** (1993) 693-695.
3. J. Y. Tsao, B. W. Dodson, Excess stress and stability of strained heterostructures. *Appl. Phys. Lett*, **53** (1988) 848-850.

S16

TOWARDS LIMITS OF X-RAY SPECULAR REFLECTIVITY

J. Jíša and M. Meduňa

Department of Condensed Matter Physics, Kotlářská, 611 37 Brno
janjisa@mail.muni.cz

In the last decades, thin film technologies found numerous applications in many physical, technological and industrial fields and are used in various procedures within research in microelectronics, optoelectronics, optics, biology and nanotechnology. The production of semiconductor devices, integrated circuits, recordable media such as optical discs and hard-discs, or special coatings and filters on optical elements are based on thin film technology. The production of thin films requires determination of their properties, which are necessary to parameterize the designed structure of the device being processed. Thickness, density, material composition, crystalline structure, refractive index and interface roughness in individual layers of the structure are typical parameters investigated during the layer growth.

In order to characterize the layers, there are many techniques for investigation of thin film properties, usually based on the interference of electromagnetic radiation. These methods covering wavelengths from infrared optics up to X-rays have an advantage of non-destructive diagnostics. Optical reflection and ellipsometry are mostly used for thick layers with thicknesses of around 1 m. On the contrary, X-ray specular reflectivity is much more sensitive to very thin layers down to 0.5 nm and roughness down to 0.1 nm [1, 2]. A disadvantage of commonly used X-ray reflectometers is the upper limit of layer thicknesses (~100 nm), determined mainly by the lower resolution of X-ray optics used in the measurement setup for x-ray reflectivity.

In this work, we investigate the thickness and roughness of thin films of photoresists produced by spin coating (centrifugal casting) on silicon wafers. This procedure, which is standardly used during the production of integrated circuits in industry, is performed inside the clean room laboratory at the Department of condensed matter physics.

The spin coating method consists of depositing a small amount of liquid photoresist on a silicon wafer and subsequent spinning of the wafer up to 1000-6000 rotations per minute. A very thin, almost homogeneous and rapidly drying up photoresist layer is formed due to centrifugal forces and surface tension of the fluid. The silicon wafer with the layer is then baked at 90 - 120 °C for 3 - 5 minutes. Such a layer proceeds into the next technological step like litography and etching, where only the illuminated or un-illuminated areas are removed, according to negative or positive photoresist used. The sequences of deposition of materials with various properties (metalization, doping, etc.) are repeated combining negative or positive photoresists and other chemical procedures during the technological steps which consequently determine the structure of the designed semiconductor device. Thus the calibration of photoresist thicknesses is very important.

Determination of the thickness from x-ray specular reflectivity utilizes the interference of x-rays reflected and transmitted at the air-layer interface and the layer-substrate interface depending on the angle of incidence [3,4]. The method is commonly used for layers where the thickness is only about 2-200 times larger than the wavelength of the used radiation (very occasionally more than 1000 times). For CuK wavelength, this gives a limit of hundreds of nm for the layer. Larger thickness can be hardly measured since the interference oscillations are suppressed by the resolution function of the monochromator, various interface roughnesses, absorption in the layer and statistical noise of the signal. In our experiment we measure layer thicknesses more than 10000 times larger than the wavelength using high-resolution diffractometer [3] and Fourier transform analysis [5, 6].

The investigated photoresist layers prepared by spin coating were first measured by optical reflection probe, which is a method also based on the interference principle, but works in the visible range of spectrum (300 - 1000 nm) and in perpendicular reflection. Thicknesses of these photoresist layers depend on the angular velocity of the spinning during the deposition and vary within the range of 1100 - 1800 nm for the positive photoresist and in the range 800 - 1000 nm for the negative one. Although these thicknesses are extremely large to be measured by standard X-ray reflectivity, we have performed X-ray specular reflectivity scans as well and obtained similar values as with the optical measurements.

The setup of the X-ray reflectivity experiment, see Figure 1, was following: X-rays leave a Cu anticathode and continue to a Göbel parabolic graded multilayer mirror where the beam is collimated and monochromatized. A further double crystal Ge 220 Bartels monochromator permits propagation of only the CuK $_1$ radiation and lowers the in-plane angular divergence down to 0.003°. Slits before the sample limit the beam to dimensions 0.3 mm 8 mm.

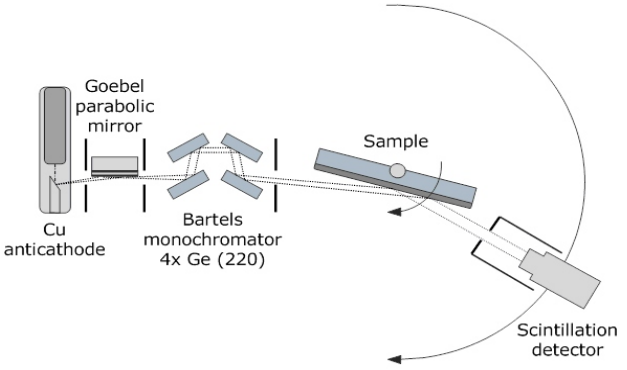

Figure 1. Schematic of the experimental setup.

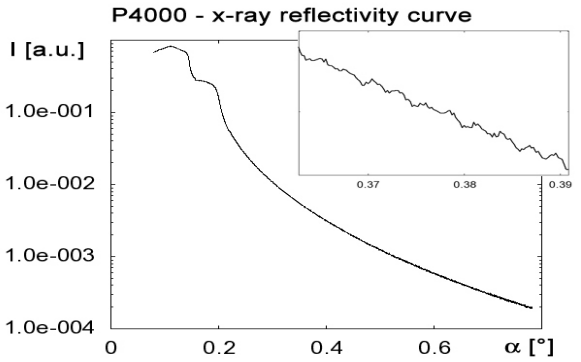

Figure 2. Measured X-ray reflectivity curve with a detail of the weak oscillations.

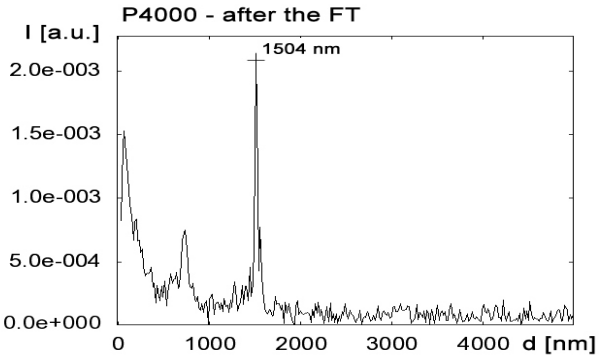

Figure 4. Fourier transform of the modified reflectivity curve in Figure 3.

Such highly collimated and monochromatic beam hits the sample at a small angle of incidence in the range of several degrees. The reflected beam propagates through the next 0.3 mm wide slit towards the scintillation detector.

The interference oscillations in X-ray specular reflectivity measurement were so weak, see Figure 2, that it is very difficult to fit the reflectivity directly by an appropriate model. Moreover, the oscillations are significantly smoothed out by the resolution function of the monochromator. Thus we used a Fourier analysis similar to the one used by authors in Refs. [5, 6]. In order to enhance the interference pattern, the measured curve was divided by a theoretical reflection of smooth silicon surface with a roughness of about 0.1-0.3 nm, see Figure 3. Parameters of this theoretical curve such as roughness, index of refraction and absorption were fitted manually in order to approximately match the measured curve. This operation enhanced the oscillations and compensated the logarithmic decay in angular space. The new curve was converted into reciprocal space (scattering vector inside the substrate) – q_z = 4 / *(sin^2($_i$)-sin^2($_c$))$^{1/2}$, where $_c$ is the critical angle for photoresist. In the next step, we could simply determine the layer thicknesses using the positions of peaks on the Fourier transformed curve, see Figure 4. The distribution of peak positions corresponds to linear combinations of possible thicknesses present within the photoresist coating deposited on the silicon surface. The position of the most intensive peak corresponds to the whole photoresist thickness.

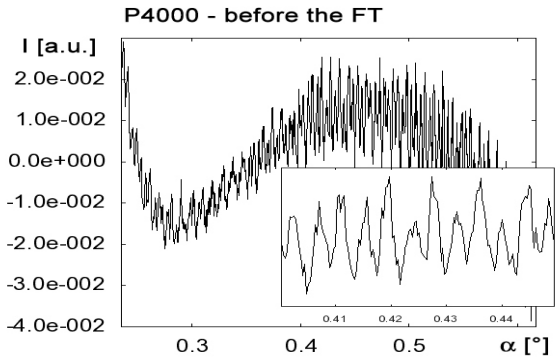

Figure 3. Reflectivity curve divided by the theoretical reflection of smooth Si surface.

Using the high resolution diffractometer we have successfully measured photoresist layers more than 1 m thick by x-rays. The thicknesses obtained by X-ray reflectivity correspond well to the ones obtained by optical reflection and the maximum deviations are about 2.3 % for positive photoresist layers and 8.5 % for negative ones.

1. P. Colombi, D. K. Agnihotri, V. E. Asadchikov, E. Bontempi, D. K. Bowen, C. H. Chang, L. E. Depero, M. Farnworth, T. Fujimoto, A. Gibaud, M.. Jergel, M. Krumrey, T. A. Lafford, A. Lamperti, T. Ma, R. J. Matyi, M. Meduna, S. Milita, K. Sakurai, L. Shabelínikov, A. Ulyanenkov, A. Van der Lee and C. Wiemer, *J. Appl. Cryst.*, **41**, (2008), 143.
2. R. J. Matyi, L. E. Depero, E. Bontempi, P. Colombi, A. Gibaud, M. Jergel, M. Krumrey, T. A. Lafford, A. Lamperti, M. Meduna, A.Van der Lee, C. Wiemer, T*hin Solid Films*, **516**, (2008), 7962
3. V.Holý, U.Pietsch, T.Baumbach, High-resolution x-ray scattering from thin films and multilay, Springer Tracts in Modern Physics, Vol.149, (Berlin: Springer) 1999, pp.120-135, 140.
4. M.Tolan, X-Ray Scattering from Soft-Matter Thin Films, Springer Tracts in Modern Physics, Vol.148, (Heidelberg: Springer) 1999.
5. K. Sakurai, A. Aida, *Jpn. J. Appl. Phys*, **31**, (1992), L113.
6. K. Sakurai, M. Mizusawa, M. Ishii, *Society of Japan* **33**, (2008), 523.

We would like to thank Václav Holý for regular thoughtful discussions and advices, Ondřej Caha for practical tips on handling an X-ray experiment, Petr Mikulík for providing the reflection probe measurement software and tutorials on the work in clean rooms and Milan Kučera for helping with depositions in the clean rooms. The work was supported by the projects 202/09/1013 of the Czech Science Foundation and MSM0021622410 of the Ministry of Education of the Czech Republic.

S17

DETERMINATION OF Mn AND P CONCENTRATION IN $Ga_{1-x}Mn_xAs_{1-y}P_y$

L. Horák[1], V. Holý[1], V. Valeš[1], C. R. Staddon[2], P. Wadley[2], R. P. Campion[2]

[1]*The Department of Condensed Matter Physics, Faculty of Mathematics and Physics, Charles University, Ke Karlovu 5, 121 16 Prague 2, Czech Republic*
[2]*School of Physics and Astronomy, University of Nottingham, Nottingham NG7 2RD, UK*
horak@karlov.mff.cuni.cz

Gallium manganese arsenide phosphate is a modification of the intensively studied magnetic semiconductor GaMnAs. There is a hope that incorporation of phosphorus could increase Currie temperature due to the stronger interaction in tighter lattice. Influence of phosphorus on concentration of interstitial manganese is another unknown and important effect. These are reasons to improve commonly used method for concentration determination in technological laboratories.

The easiest X-ray approach to determine a concentration of $Ga_{1-x}Mn_xAs_{1-y}P_y$ quaternary is a comparison of measured lattice parameters with computed ones from Vegard's law. For this purpose, the tabulated parameters for GaAs and GaP are used. MnAs and MnP is not natively zinc-blend structure, lattice parameters for MnAs(Z-B) and MnP(Z-B) are extrapolated from the X-ray measurements of ternaries with known content from the growth. One lattice parameter is given by two unknown values of concentrations; we have to measure only special series of samples to have the same number of measured parameters and unknown concentration, e.g. the series with the same concentration of P including one sample with no Mn content.

We present a method of concentration determination based on comparison of simulated and measured diffraction curves. For computation of simulated curve the structure factor is used, which is affected by element concentrations. The influence on the structure factor differs for substitutional and interstitial atoms. The dependence of the structure factor on expansion coefficients (relation between concentration and lattice parameter) is very weak. Those coefficients are not very known today and meaning of concentration used in experimental calibration curve is unclear; this is the main advantage of this approach.

The change of intensity with a different concentration can be observed for the so-called weak diffractions. These diffractions are very sensitive to Mn and P content, because contributions of Ga and As atoms to the structure factor have the opposite phase but the similar amplitude. This is demonstrated by Figure 1, which shows a simulated diffraction curve for three diffractions with varying phosphorus concentration from 0% to 30%. The curve for strong diffraction (004) differs only by the peak position, which corresponds to the different lattice parameter, whereas peak intensity is strongly dependent on the concentration in case of weak diffractions (002) and (006). Interesting fact can be derived from this plot; there is a specific concentration of phosphorus, which makes structure factor of GaAsP zero, and in this case, the pure Mn contribution to structure factor can be measured.

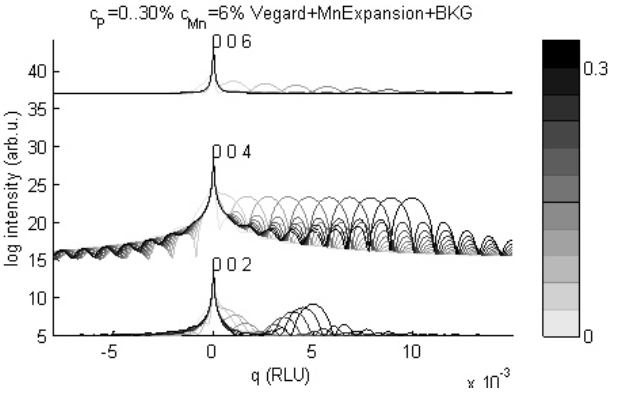

Figure 1. Simulated diffraction curves, concentration of phosphorus goes from 0 to 30 %.

The substitutional manganese has very small effect on lattice parameter, which is not quantified yet. Figure 2 shows the shift of peak for (004) which is not sufficient to determine anything, but intensity of (002) diffraction changes rapidly while there is no significant shift.

There are two types of interstitial positions; manganese can be positioned inside of gallium (or arsenic) tetrahedron. Unfortunately, they compensate each other their effect on structure factor for weak diffraction and contribution is too small for strong diffraction. It is case of diamond lattice for the same occupancy where weak diffraction turns to forbidden. We can estimate only the difference of those occupancies from structure factor, the absolute values are surely included in lattice parameter, but we do not know expansion coefficients again.

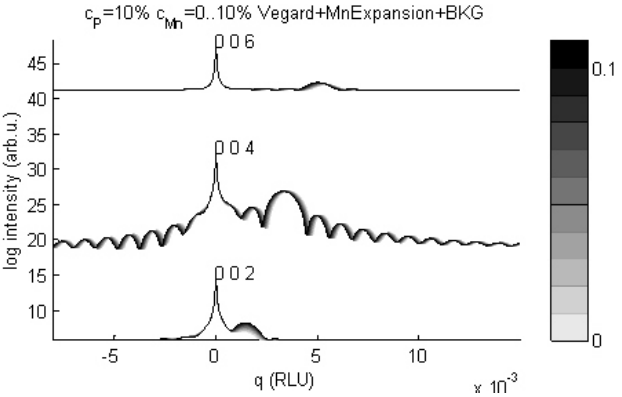

Figure 2. Concentration of substitutional Mn goes from 0 to 10%

The number of parameters increases with sensitivity to positions of atoms in the lattice. It is obvious that there is no extra information about lattice parameter for different diffractions, while structure factors differ. We should measure many diffractions to determine concentration properly, but our task was to develop method for rapid laboratory characterization of grown samples. For some instrumental reasons it is necessary to measure reciprocal space maps, not only line scans over substrate and layer peak. If we take into account, that intensity of weak diffraction is very low, those measurements are very time consuming. It is important to find fast method for standard laboratories with no main focus on x-ray and many samples to characterize. We measure only two diffractions (002) and (004), which takes at least 3 days. To solve problem of many parameters we use the control samples with the same phosphorus concentration and no manganese. The assumption of equal concentration is reasonable, control samples are grown anyway within the growing procedure.

The dynamic scattering theory is used to simulate diffraction curves. It is possible to determine concentrations, but there are still problems with numerical instability of optimizing algorithm. To get unique solution one has to use simply model such as homogeneous layer with some fixed parameters (e.g. concentration of As antisites). The aim of this work is to develop a reliable robust method for characterization in a technological laboratory. Latest progress and conclusions will be presented in the talk.

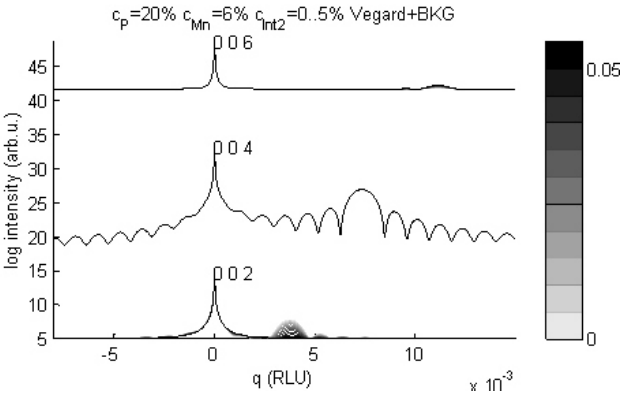

Figure 3. Difference of interstitial Mn concentration goes from 0 to 0.05

S18

STANDING-WAVE-GRAZING-INCIDENCE X-RAY DIFFRACTION FROM POLYCRYSTALLINE MULTILAYERS

J. Krčmář[1], V. Holý[2], I. Vávra[3]

[1]*Institute of Condensed Matter Physics, Masaryk University, Koltářská 2, 611 37 Brno, Czech Republic*
[2]*Department of Physics of Electronic Structures, Charles University, Ke Karlovu 5, 121 16 Prague, Czech Republic*
[3]*Institute of Electrical Engineering Slovak Academy of Sciences, Dúbravská cesta 9, 84239 Bratislava, Slovak Republic*
krcmar@physics.muni.cz

In work [1] authors presented a new diffraction method, which uses the concept of X-ray standing wave in the grazing-incidence geometry, in which both the incidence and exit angles $_{i,f}$ are close to the critical angle $_c$ of total external reflection. If the angle of incidence $_i$ of the primary X-ray wave onto a periodic multilayer is close to $_i$ or to a "Bragg-like" maximum on the reflectivity curve, the interference of the transmitted and reflected waves creates a standing wave pattern in the multilayer volume, the period of which equals the multilayer period. If the multilayer contains crystalline grains (crystallites), the intensity of diffraction from these crystallites depends on the mutual position of the crystallites and the antinodes of the standing wave. Similarly, the wave diffracted by the crystallites is reflected from the multilayer interfaces, which results in a standing wave pattern as well. The standing wave pattern is shifted by changing $_i$ or $_f$ so that from the measured dependence of the diffracted intensity on $_{i,f}$ it is possible to determine the position of the diffracting crystallites. Moreover, measuring the dependences of the diffracted intensity on the in-plane scattering angle 2 at various $_i$ it is possible to determine the lateral sizes of the crystallites in different depths in the multilayer. The theoretical description of the scattering process is based on the Distorted-Wave Born approximation.

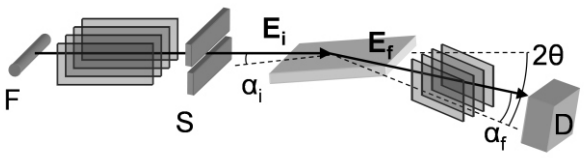

Figure 1. The geometry of the experimental method in the laboratory. X-ray tube has line focus F parallel to the surface plane. The incident E_i beam is restricted by a parallel plate collimator and slit S. The scattered beam E_f is restricted by a second parallel plate collimator. 2 is the scattering angle and $_i$ and $_f$ are the incident and exit angles with respect to the sample surface.

In Ref. [2], we proved the feasibility of this concept by measuring the standing-wave effects in C/Ni_3N multilayers using synchrotron radiation, and we were able to determine the sizes of the crystallites in different depths in the multilayer and the thicknesses of amorphous Ni_3N transition layers at the C/Ni_3N interfaces.

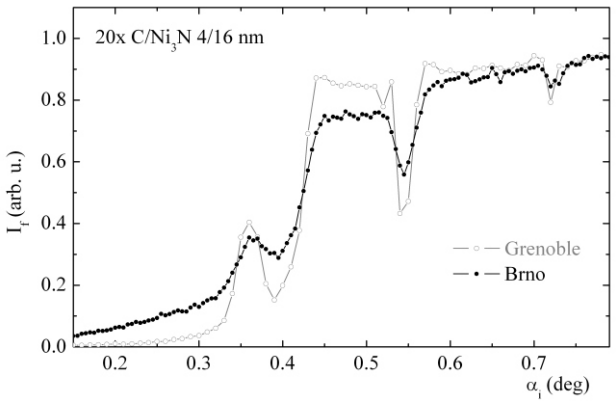

Figure 2. Diffraction measured in the laboratory (Brno) and at the ID01 beamline at ESRF (Grenoble).

In Ref. [3], we demonstrate that this method can be carried out also at a modified X-ray diffractometer (Figure (1)), and it is capable of studying the structure of crystalline layers in a periodic multilayer at a laboratory (Figure (2)). We have used this method for the investigation of the structure of Nb/Si multilayers, and we obtained the thicknesses of amorphous and crystalline parts of the Nb layers. These thicknesses agree very well with the transmission electron microscopy observations.

From the fits, it follows that the Nb layer consists in an amorphous part of the thickness of 2.0±0.5 nm lying at the Si/Nb interface (i.e., in the bottom part of the Nb layer) and of the crystalline part in the upper part of the layer at the Nb/Si interface. Figure (3) shows the comparison of the measured and fitted intensity curves. To demonstrate the sensitivity of the method, in Fig. (3) we have also plotted the calculated diffraction curves assuming that whole Nb layers are crystalline (dashed lines). From the figure, it is obvious that the agreement of these curves with the experimental data is much worse and the method is capable indeed to measure the thickness of the amorphous part of the Nb layer.

Presented method is very suitable for a detailed study of sizes and positions of crystallites in periodic multilayers, as well as for the determination of the depth profile of the crystallite size.

1. P. F. Fewster, N. L. Andrew, V. Holý, K. Barmak, *Phys. Rev. B*., **72**, (2005) 174105.
2. J. Krčmář, V. Holý, L. Horák, T. H. Metzger, J. Sobota, *J. Appl. Phys*., **103**, (2008) 033504.
3. J. Krčmář, V. Holý, I. Vávra, *Appl. Phys. Lett*., **94**, (2009) 101909.

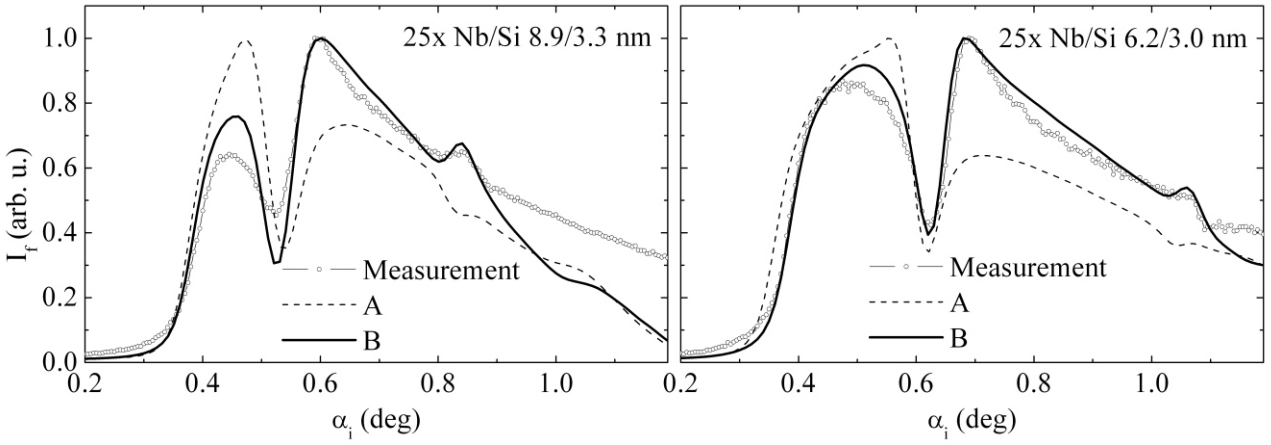

Figure 3. Measured (points) and fitted (lines and dash line) diffraction intensities. Curve A: all volume of Nb layers is crystalline. Curve B: bottom 2 nm thick parts of the Nb layers are amorphous.

S19

DETERMINATION OF PRECIPITATE CONCENTRATION USING LAUE DIFFRACTION

S. Bernatová, O. Caha

Institute of Condensed Matter physics, Masaryk University, Kotlářská , 611 37 Brno, Czech Republic
author@muni.cz

Structural quality of semiconductor wafers and epitaxial layers is an important parameter substantially influencing their electrical properties and the performance of fabricated integrated circuits. A reliable control of the defect nucleation and growth during the semiconductor technology is an important issue, since the defects may affect detrimentally the electric parameters of the semiconductor structures, but they can also be beneficial, because they can getter out impurities, especially heavy metal atoms.

The x-ray scattering methods, especially diffuse scattering around reciprocal lattice points, were often used in past for the defect characterization. The diffuse scattering provides us the information about precipitate shapes, sizes and deformation field around them. However, the determination of their absolute concentration is not straightforward; the diffuse scattered intensity from the defects has to be normalized, for instance to the thermal diffuse scattering [1]. This drawback can be overcome by measurement of the rocking curve in a two-crystal setup without analyzer,

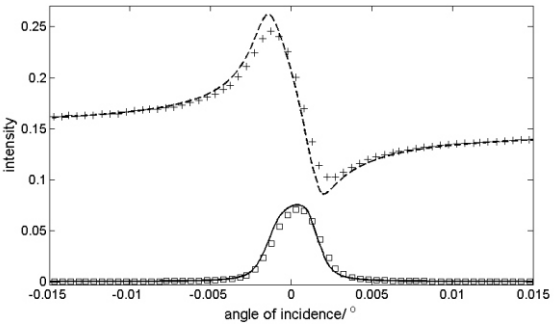

Figure 1. The dependence of the diffracted (squares) and transmitted (crosses) intensity on the angle of incidence in 220 diffraction on a float zone (defect free) silicon crystal. The measured intensity is compared to the theoretical diffraction curves (dashed and solid lines). The angle of incidence is measured with respect to the Bragg position.

which can be normalized directly to the intensity of the primary beam. This method was used in the Bragg diffraction geometry by several authors [2]. We have used the Laue geometry, which allows us to measure both the diffraction curve and the transmission curve simultaneously, and therefore gives us more information.

We have used X-ray diffractometer with Cu tube and germanium 220 Bartels (4 crystal) monochromator without analyzer. We have checked the diffractometer angular resolution on a float zone (defect free) silicon crystal. The sample was polished and etched to the thickness of 0.122 mm. The measured diffraction and transmission curves are shown in the figure 1. The experimental curves were compared with the dynamical theory of X-ray diffraction

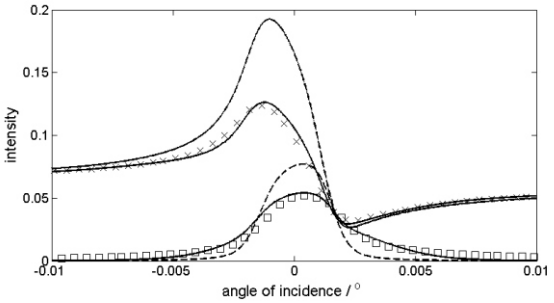

Figure 2. The dependence of the diffracted (squares) and transmitted (crosses) intensity on the angle of incidence in 220 diffraction on the sample with precipitates. Thin line shows the calculation of diffracted intensity, dotted line shows the calculation of transmitted intensity, by the statistical dynamical theory of x-ray diffraction and. Dot-and-dash line and dash line show curves of the perfect crystal.

[3]. The slight disagreement of the theoretical and experimental dependences can be explained by inhomogeneity in the sample thickness.

The sample of a Czochralski grown silicon underwent a three stage annealing process (600°C/8 h, 800°C/4 h and 1000°C/16 h). The sample was polished and etched to the thickness 0.180 mm. The experimental diffraction and transmission curves strongly differs from the theoretical diffraction curves of ideal crystal, see figure 2. Especially, the intensity of the transmitted beam is much lower than from an ideal crystal. The diffraction profiles of the defected crystal was calculated using statistical dynamical theory [4], where the defects were assumed as amorphous spheres randomly displaced inside the crystal lattice. The best coincidence was found for the precipitate radius 1.2 m and their volume ratio of 3%, which corresponds to the absolute precipitate concentration of $0.9 \cdot 10^{10} cm^{-3}$.

1. L. A. Charni, K. D. Scherbachev, V. T. Bublik, *phys. stat. sol. (a)* ***99***, (1991), 267.
2. V. B. Molodkin, S. I. Olikhovskii, E. N. Kislovskii, T. P. Vladimirova, E. S. Skakunova, R. F. Seredenko, B. V. Sheludchenko, *Phys. Rev. B* ***78*** (2008), 224109.
3. see for instance A. Authier, *Dynamical theory of x-ray diffraction*, (Oxford university press, 2001).
4. V. Holý & K. T. Gabrielyan, *phys. stat. sol. (a)* ***140***, (1987), 39.

The authors would like to acknowledge prof. V. Holý for providing the simulation code.

S20

X-RAY SCATTERING ON GaN THIN FILMS, MONTE CARLO SIMULATION

M. Barchuk[1], V. Holý[1], B. Miljevic[2], B. Krause[2]

[1]Charles University in Prague, Faculty of Mathematics and Physics, Ke Karlovu 5, 12116 Praha 2, Czech Republic;
[2]Forschungszentrum Karlsruhe GmbH, Institute for Synchrotron Radiation, Hermann-von-Helmholtz-Platz 1, D-76344 Eggenstein-Leopoldshafen, Germany

Gallium nitride (GaN) is a most promising material for the base of photonic devices (LED and laser diodes, daylight visible full-color LED displays etc.). We investigate the defect structure of GaN epitaxial layers deposited by metalorganic vapor-phase deposition (MOVPE) on c-oriented sapphire substrates (Al_2O_3) covered by a thin AlN nucleation layer. The aim of our study is to determine the density of threading dislocations penetrating through the layer thickness towards free surface.

The large lattice mismatch between the GaN epitaxial layer and the applied substrate has a large influence upon the dislocation density increasing it to the order of 10^9 cm^{-2}. The dislocation density can be reduced by in-situ deposition of a SiN_X intermediate layer with sub-monolayer coverage [1]. This layer acts as a self-organized mask partially pinning the threading dislocations propagating from the substrate interface.

We used diffuse X-ray scattering in coplanar (0004) diffraction, the experiments were carried out at ANKA (Karlsruhe, Germany) on a 6-circle diffractometer at SCD beam-line over a samples series with various nominal thickness of the SiN pinning layer, the nominal thickness of GaN was between 1.8 to 2.4 m, the sample description is given in Table 1. Depending on the thickness of the SiN

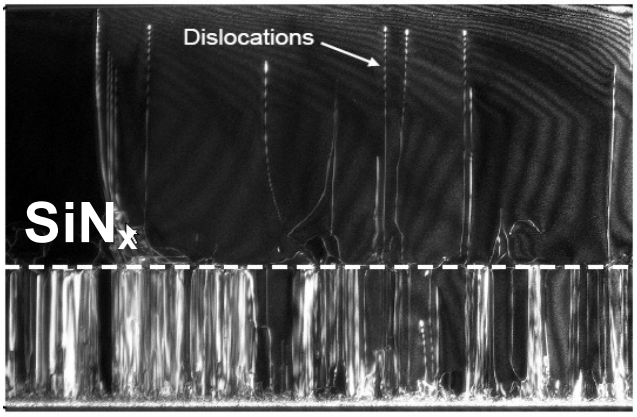

Figure 1. Transmission electron micrograph of the sample cross-section (Hertkorn J. et al, Uni-Ulm).

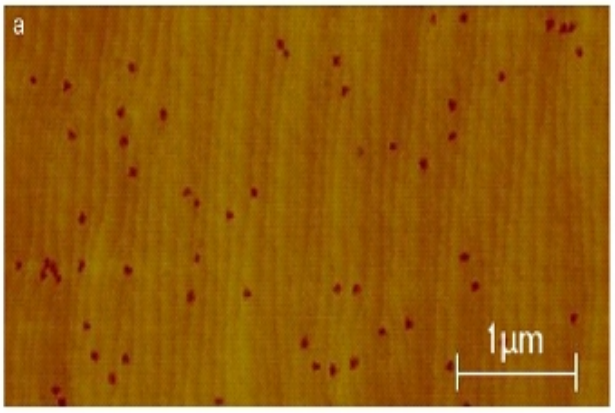

Figure 2. Etched GaN surface, the etch pits correspond to individual dislocations. (Martin Beer, Uni-Regensburg).

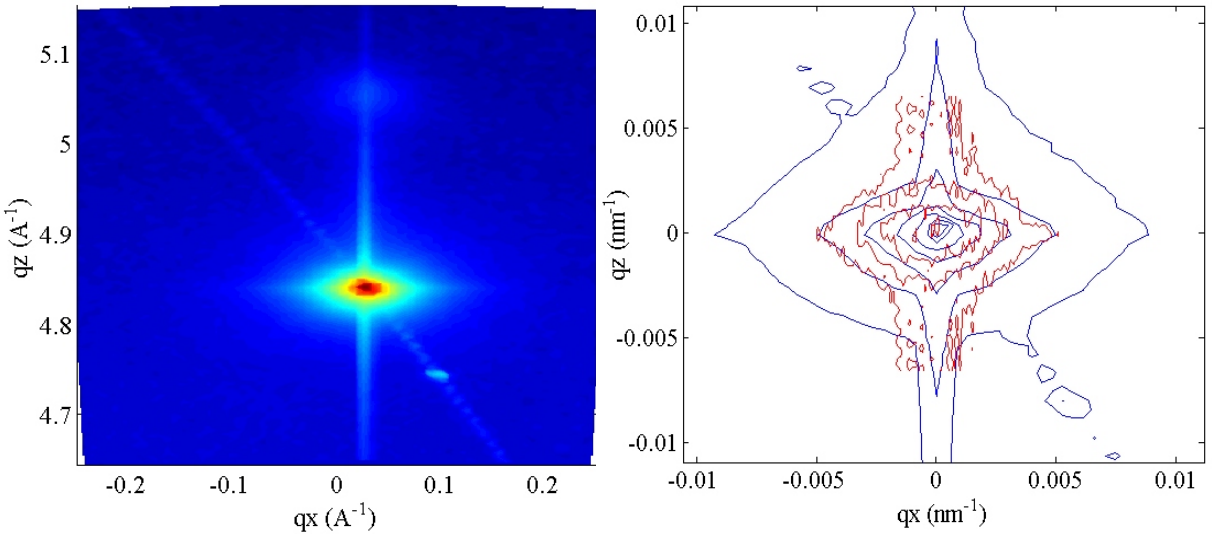

Figure 3. Experimental RSM of the sample S8134 in (0004) diffraction (a) and the comparison measured (blue) and simulated (red) intensity distributions (b).

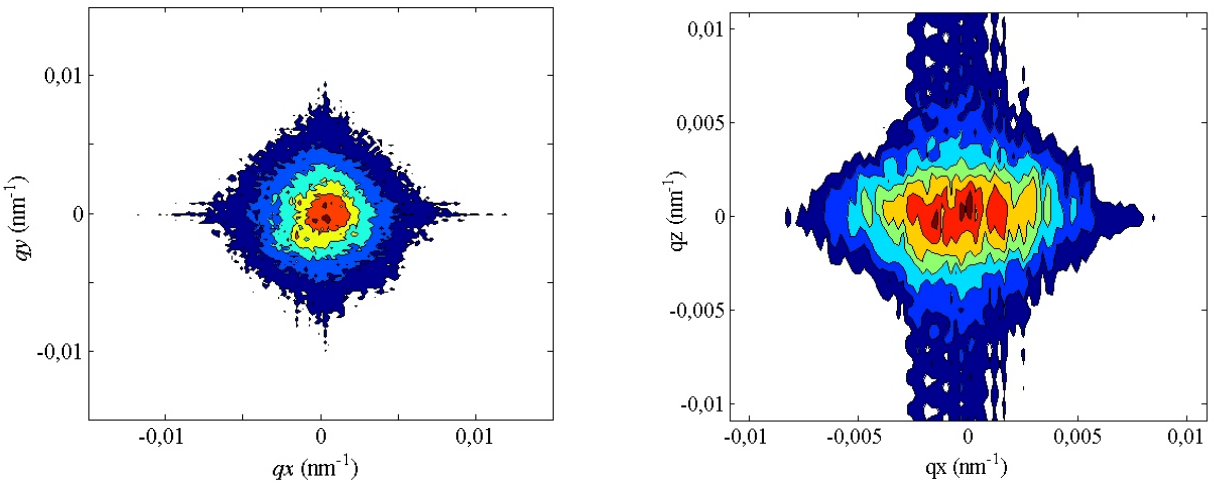

a) b)

Figure 4. Simulated RSMs for screw (a) and edge (b) threading dislocations in (0004) diffraction for the sample with the lowest dislocation density (S8134). The proportion between screw and edge dislocation densities is 1:10.

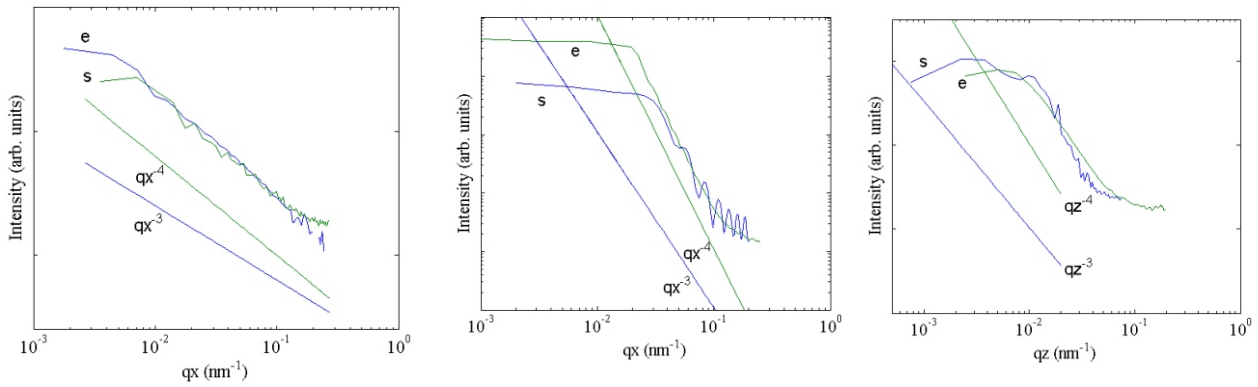

Figure 5. Cuts of RSMs for screw (a) and edge (b)-(c) dislocation types in log-log representation, symbols **e** and **s** denote experimental and simulated curves, respectively.

interlayer one could obtain different densities of threading dislocation that allowed us to get a sufficient set of experimental data (reciprocal space maps - RSM), radial and rocking curves, reflectivity measurements) and apply it for comparison with simulated ones.

The approximate defect density in these samples was estimated by transmission electron microscopy (TEM – see Fig. 1) and from the etch pit density (Fig. 2). Coincidence between these densities and the density following from our X-ray measurements is a proof of our theoretical approach for the defect description.

Figure 3 (a) presents an example of a measured reciprocal-space distribution of X-ray intensity diffusely scattered in symmetric diffraction 0004. Two maxima correspond to the AlN nucleation layer (the upper weak maximum) and to the GaN epitaxial layer (the strong maximum at q_z Å^{-1}).

Diffuse X-ray scattering from defects can be described by conventional Krivoglaz theory [2]. In our case this approach is not suitable because its numerical implementation for threading dislocations contains very complicated integrals. Therefore, we applied a Monte-Carlo simulation instead.

We generated random positions and types of threading dislocations, including a correlation in their positions, then we calculated the displacement field caused by the dislocations and the non-averaged amplitude of the scattered wave [3]. Performing a statistical average we obtained the scattered wave distribution in reciprocal space, i.e., the reciprocal space maps for different dislocation types (see characteristic examples in Fig. 4).

From the set of experimental RSMs in symmetrical (0004) diffraction we could separate the contributions from pure screw and edge dislocations. In contrast to the screw threading dislocation, the edge ones appreciably contributed to intensity distribution in the *qx*-*qz* plane. Our main goal is to compare simulated and measured RSMs and their main cuts (Fig.3 (b)). Plotting both experimental and simulated cuts through the reciprocal-space intensity distribution along *qx* and *qz* axes in log-log representations (Fig.5) we are able to investigate the asymptotic behavior of the tails of the intensity profiles and to gain information about

Table 1. The sample parameters

Name of the sample	SiN_x deposition time, [s]	Dislocation density (EPD), $*10^8$ [cm^{-2}]	Screw dislocation density from simulations, $*10^8$ [cm^{-2}]	Edge dislocation density from simulations, $*10^8$ [cm^{-2}]	Total dislocation density from simulations, $*10^8$ [cm^{-2}]
	180	2.6	0.3 ± 0.1	2.7 ± 1.1	3 ± 1.2
S8135	150	4.8	-	-	5.0 ± 1.5
S8136	120	7.6	-	-	7.5 ± 2.2
S8071	0	20	2 ± 0.6	21.5 ± 6	23.5 ± 6.5

the prevailing dislocation type [4]. The estimated dislocation densities from our simulations are given in Table 1.

A detailed analysis demonstrates that the Monte-Carlo method can be used for the calculation of diffuse scattering from dislocations in epitaxial layers. For GaN layers in particular, this analysis makes it possible to determine the densities of individual types of dislocations.

1. Hertkorn J. et al., *J. Crystal Growth* **308**, 30-36 (2007).
2. M.A. Krivoglaz, X-Ray and Neutron Diffraction in Nonideal Crystals, *Mater. Sci. Eng.*, **A 49** (2001);
3. S.J. Shaibani and P.M. Hazzledine, *Phyl. Magazine* **A**, 1981, Vol. **44**, No.3, 657-665.
4. V.M. Kaganer, O. Brandt, A. Trampert and K.H. Ploog, *Phys. Rev.* **B 72**, 045423 (2005).